J|A|C|S
ARTICLES
Published on Web 04/03/2003

Great Structural Variety of Complexes in Copper(II)−Oligoglycine Systems: Microspeciation and Coordination Modes as Studied by the Two-Dimensional Simulation of Electron Paramagnetic Resonance Spectra

Nóra Veronika Nagy,[†] Terézia Szabó-Plánka,*[,†] Antal Rockenbauer,[‡] Gábor Peintler,[†] István Nagypál,[†] and László Korecz[‡]

Contribution from the Department of Physical Chemistry, University of Szeged, P.O. Box 105, H-6701 Szeged, Hungary, and Chemical Research Center, Institute of Chemistry, Hungarian Academy of Sciences, P.O. Box 17, H-1525 Budapest, Hungary

Received October 3, 2002

Abstract: A series of isotropic EPR spectra recorded at various concentrations and pH (in the range 2−12) on equilibrium systems containing copper(II) and diglycine, triglycine, or tetraglycine were analyzed. A purely mathematical method, matrix rank analysis gave the number of independent EPR-active species. Two-dimensional evaluation then resulted in the formation constants and magnetic parameters of 14 metal complexes (including microspecies) in each system. The independent paramagnetic species formed with each ligand are as follows: Cu^{2+} (aqua complex), $[CuLH]^{2+}$, $[CuL]^{+}$, $[CuLH_{-1}]$, $[CuLH_{-2}]^{-}$, $[CuL_2H_2]^{2+}$, $[CuL_2H]^{+}$, $[CuL_2]$, $[CuL_2H_{-1}]^{-}$, and $[CuL_2H_{-2}]^{2-}$. Moreover, for diglycine, the diamagnetic complex $[Cu_2L_2H_{-3}]^{-}$, and for triglycine and tetraglycine, the EPR-active species $[CuLH_{-3}]^{2-}$ were identified. Further, equilibria of two microspecies were demonstrated for $[CuL_2]$, $[CuL_2H_{-1}]^{-}$, and $[CuL_2H_{-2}]^{2-}$. The magnetic parameters allowed a detailed description of the coordination modes. The most important findings: (1) For the *mono* complexes, the in-plane σ-bonds between copper(II) and the equatorial N donors are particularly strong when the same ligand forms several adjacent chelate rings with the participation of amino N, deprotonated peptide N(s), and the carboxylate group. (2) Structures with coupled chelate rings are likewise favored in the bis complexes. Different protonation states of the two ligands are observed in the major isomer of $[CuL_2]$ ($(LH_{-1} + LH)$ coordination), and in the isomers of $[CuL_2H_{-2}]^{2-}$ ($(LH_{-2} + L)$ coordination) for triglycine and tetraglycine.

Introduction

We recently developed an integrated EPR-spectroscopic method[1] with which to elucidate the microspeciation and the corresponding coordination modes for overlapping equilibria in multispecies paramagnetic systems. Our "two-dimensional" evaluation method involves the simultaneous analysis of series of EPR spectra recorded at various metal and ligand concentrations and pH. It gives the formation constants of both the paramagnetic species (including microspecies, i.e., isomers) and the diamagnetic metal complexes; simultaneously, it furnishes the magnetic parameters of the EPR-active species, which yield information on the nature of the coordinating groups and additional details concerning the coordination modes.

As the oligoglycines are good models with which to study the coordinating abilities of backbone donor groups in proteins, the copper(II)−triglycine and copper(II)−tetraglycine systems have been extensively investigated during recent decades.[2−8] Their superoxide dismutase-like activity has been demonstrated.[9] In various pH potentiometric and visible spectroscopic studies, attention has mainly been focused on the stability and structure of the mono complexes which predominate at equal metal and ligand concentrations. The anchoring role of the terminal amino N atom and simultaneous binding of the neighboring peptide group (by the O atom at low pH, and then by the deprotonated N atom at some higher pH), followed by stepwise proton loss and the coordination of further peptide groups with increasing pH, are generally accepted.[2−8] The speciation and particularly the coordination modes at a ligand excess are much less well understood. An interesting question that is difficult to solve is the competition between the two ligands for the equatorial sites of the metal ion in bis complexes. In some cases, both

[†] Department of Physical Chemistry, University of Szeged.
[‡] Chemical Research Center, Institute of Chemistry, Hungarian Academy of Sciences.

(1) Rockenbauer, A.; Szabó-Plánka, T.; Árkosi, Zs.; Korecz, L. *J. Am. Chem. Soc.* **2001**, *123*, 7646−7654.
(2) Kim, M. K.; Martell, A. E. *J. Am. Chem. Soc.* **1966**, *88*, 914−918.
(3) Hanaki, A.; Kawashima, T.; Konishi, T.; Takano, T.; Mabuchi, D.; Odani, A.; Yamauchi, O. *J. Inorg. Biochem.* **1999**, *77*, 147−155.
(4) Sóvágó, I.; Sanna, D.; Dessi, A.; Várnagy, K.; Micera, G. *J. Inorg. Biochem.* **1996**, *63*, 99−117.
(5) Brookes, G.; Pettit, L. D. *J. Chem. Soc., Dalton Trans.* **1975**, 2106−2111.
(6) Martin, R. B.; Mosoni, L.; Sarkar, B. *J. Biol. Chem.* **1971**, *246*, 5944−5947.
(7) Bal, W.; Kozlowski, H.; Lisowski, M.; Pettit, L. D. *J. Inorg. Biochem.* **1994**, *55*, 41−45.
(8) Sigel, H.; Griesser, R.; Prijs, B. *Z. Naturforsch.* **1972**, *B27*, 353−358.
(9) Pogni, R.; Baratto, M. C.; Busi, E.; Basosi, R. *J. Inorg. Biochem.* **1999**, *73*, 157−165.

10.1021/ja021245+ CCC: $25.00

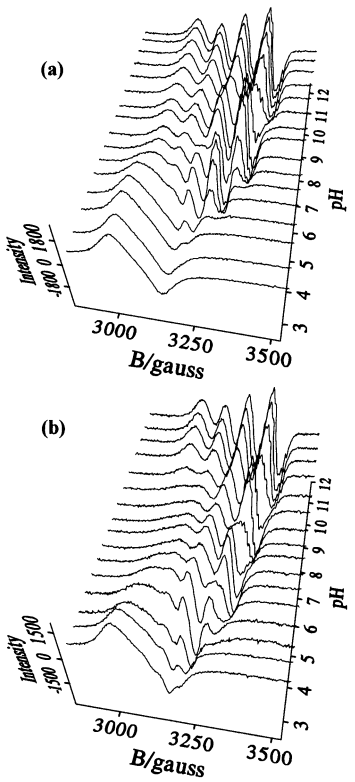

Figure 1. Series of experimental EPR spectra for the copper(II)−tetraglycine system; (a) $T_{Cu} = T_L = 5$ mM and (b) $T_{Cu} = 5$ mM, $T_L = 75$ mM.

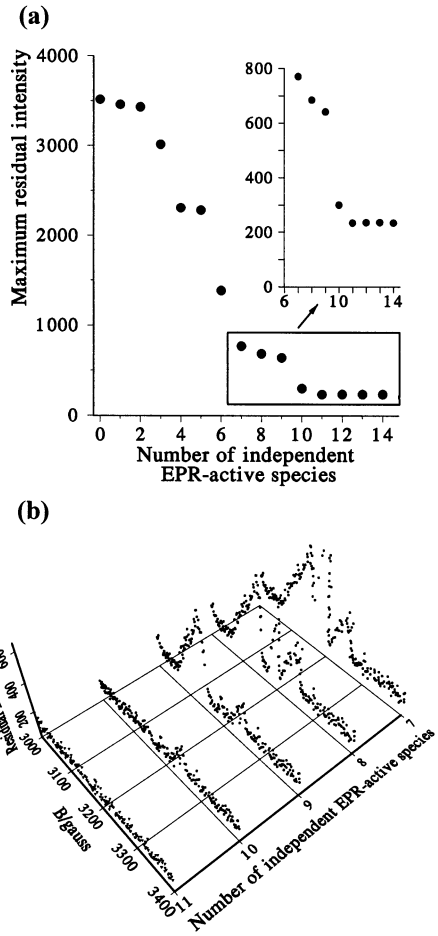

Figure 2. Results of matrix rank analysis on the whole series of spectra for the copper(II)−tetraglycine system; (a) maximum residual intensity values and (b) residual intensity curves for different numbers of EPR-active species.

oligoglycine ligands may occupy two equatorial positions via the same donors (e.g., (L + L) binding in $[CuL_2]$ or (LH_{-1} + LH_{-1}) coordination in $[CuL_2H_{-2}]^{2-}$); however, different protonation states and coordination modes of the two ligands cannot be excluded (((LH_{-1} + LH) or (LH_{-2} + L) binding mode, respectively). The above coordination modes may coexist in various microspecies, and geometric isomerism may also occur. Apart from potentiometric and spectrophotometric methods, EPR spectroscopy offers a possibility for the distinction and characterization of microspecies, so it has long been used to study isomeric equilibria of predominant copper(II) complexes by analysis of the N superhyperfine splitting in the high-field region of the spectra.[10] However, pH potentiometric data[3−8] indicate that the bis complexes of either triglycine or tetraglycine are not formed exclusively under any conditions, and their investigation by the unique decomposition of the spectra therefore requires the simultaneous analysis of series of experimental curves.

In the present paper, we report results obtained by two-dimensional simulation of the EPR spectra of the copper(II)−triglycine and copper(II)−tetraglycine systems, together with those of the better-known copper(II)−diglycine system.[11−14] In the latter case, the coordination at ligand excess seems to be an open question. We aimed to utilize the selectivity of EPR spectroscopy to identify possible isomer pairs, to determine the donor groups involved in the coordination, and to obtain information about the metal−ligand bonds and the local geometry around the copper ion.

Results and Discussion

Number of Independent Species in the Copper(II)−Oligoglycine Systems. Recent publications[4−6] have described numerous mono and bis complexes in the copper(II)−oligoglycine systems, but even more independent species can reasonably be assumed. For the sake of easier two-dimensional analysis, therefore, it seemed necessary to clarify beforehand how many independent EPR-active species are formed in our solutions. Accordingly, the whole series of spectra were first evaluated by matrix rank analysis, a model-free mathematical method.[15] The experimental EPR curves for the copper(II)−tetraglycine system are shown in Figure 1. Figure 2 illustrates for the same series of spectra that (a) the maximum residual intensity is

(10) (a) Goodman, B. A.; McPhail, D. B.; Powell, H. K. J. *J. Chem. Soc., Dalton Trans.* **1981**, 822−827. (b) Goodman, B. A.; McPhail, D. B. *J. Chem. Soc., Dalton Trans.* **1985**, 1717−1718. (c) Valensin, G.; Basosi, R.; Antholine, W. E.; Gaggelli, E. *J. Inorg. Biochem.* **1985**, *23*, 125−130. (d) Pasenkiewicz-Gierula, M.; Froncisz, W.; Basosi, R.; Antholine, W. E.; Hyde, J. S. *Inorg. Chem.* **1987**, *26*, 801−805. (e) Pogni, R.; Della Lunga, G.; Basosi, R. *J. Am. Chem. Soc.* **1993**, *115*, 1546−1550.

(11) Shtyrlin, V. G.; Gogolashvili, E. L.; Zakharov, A. V. *J. Chem. Soc., Dalton Trans.* **1989,** 1293−1297.

(12) (a) Gergely, A.; Nagypál, I. *J. Chem. Soc., Dalton Trans.* **1977,** 2106−2109. (b) Farkas, E.; Kiss, T. *Polyhedron*, **1989**, *8*, 2463−2467.

(13) Kittl, W. S.; Rode, B. M. *J. Chem. Soc., Dalton Trans.* **1983**, 409−414.

(14) (a) Sheinblatt, M.; Becker, E. D. *J. Biol. Chem.* **1967**, *242*, 3159−3164. (b) Kozlowski, H. *Chem. Phys. Lett.* **1977**, *46*, 519−520. (c) Sato, M.; Matsuki, S.; Ikeda, M.; Nakaya, J. I. *Inorg. Chim. Acta* **1986**, *125*, 49−55. (d) Szabó-Plánka, T.; Rockenbauer, A.; Korecz, L. *Magn. Reson. Chem.* **1999**, *37*, 484−492.

(15) Peintler, G.; Nagypál, I.; Jancsó, A.; Epstein, I. R.; Kustin, K. *J. Phys. Chem. A* **1997**, *101*, 8013−8020.

Table 1. Formation Constants as log β[a] for the Copper(II) Complexes of Diglycine, Triglycine, and Tetraglycine

	ligand[b]												
	diglycine				triglycine					tetraglycine			
complex	this work	ref 11	ref 12	ref 13	this work	ref 3	ref 4	ref 5	ref 6	this work	ref 4	ref 7	ref 8
$[CuLH]^{2+}$	9.42(8)	9.36			9.47(9)		9.51		9.65	9.56(7)	9.09		
$[CuL]^{+}$	5.60(3)	5.63	5.56	5.62	5.26(5)	5.08	5.25	5.13	5.30	5.07(3)	5.06	5.07	5.08
$[CuLH_{-1}]$	1.36(1)	1.24	1.33	1.45	0.06(3)	−0.03	−0.16	−0.05	−0.18	−0.48(2)	−0.50	−0.54	−0.42
$[CuLH_{-2}]^{-}$	−8.10(1)	−8.28	−8.04	−8.09	−6.77(3)	−6.76	−7.02	−6.77	−6.97	−7.32(1)	−7.41	−7.47	−7.31
$[CuLH_{-3}]^{2-}$					−18.76(9)	−18.66	−18.30	−18.18		−16.60(2)	−16.59	−16.78	−16.6
$[CuL_2H_2]^{2+}$	18.2(1)				18.09(8)					18.00(9)			
$[CuL_2H]^{+}$	14.5(1)				14.19(6)					14.40(6)			
$[CuL_2]$	10.04[c]				9.32[c]			9.6	9.66	9.17[c]			
LH_{-1},LH	9.9(1)				9.13(9)					9.03(5)			
L,L	9.48(7)				8.86(7)					8.60(5)			
$[CuL_2H_{-1}]^{-}$	4.51[d]	4.34	4.46	4.56	3.57[d]		3.23	2.9	3.34	3.38[d]	3.31		
isomer 1	4.34(2)				3.37(2)					2.98(2)			
isomer 2	4.03(3)				3.14(3)					3.16(3)			
$[CuL_2H_{-2}]^{2-}$	−6.83[d]	−7.70	−7.14		−4.64[d]				−4.62	−4.94[d]	−5.00		
isomer 1	−7.12(2)				−4.82(4)					−5.08(1)			
isomer 2	−7.14(5)				−5.10(7)					−5.49(4)			
$[Cu_2L_2H_{-3}]^{-}$	−4.57(8)	−4.65	−4.51	−4.63									

[a] The confidence intervals (3σ) of the last digit at a significance level of 99.7% are given in parentheses. [b] For the proton complexes [LH] and $[LH_2]^{+}$,log β values of 8.15 and 11.35 from ref 11 for diglycine, 7.93 and 11.25 from ref 4 for triglycine, and 7.94 and 11.18 from ref 4 for tetraglycine were used.[c] log $\beta = \log(\beta_{LH-1,LH} + \beta_{L,L})$. [d] log $\beta = \log(\beta_{isomer\ 1} + \beta_{isomer\ 2})$.

gradually reduced as more and more EPR-active complexes are taken into consideration, and it reaches the value of noise at 11 independent species; (b) the decrease in the residual intensities at various fields is systematic; the last small peak (near 3200 G) diminishes with the eleventh absorbing species. For triglycine as ligand, the results are similar. In the case of the copper(II)−diglycine system, the residual intensities definitely decrease up to 9 paramagnetic particles, whereas there is no significant difference if 9 or 10 absorbing complexes are taken into consideration.

Macrospeciation in the pH Range 2−12. An equilibrium model which takes into account all mono and bis complexes with reasonable protonation states in the region pH = 2−12 is in accordance with the matrix rank analysis results: it can be built up from 11 independent species for the copper(II)−triglycine and −tetraglycine systems. Accordingly, the EPR-active complexes Cu^{2+} (aqua complex), $[CuLH]^{2+}$, $[CuL]^{+}$, $[CuLH_{-1}]$, $[CuLH_{-2}]^{-}$, $[CuLH_{-3}]^{2-}$, $[CuL_2H_2]^{2+}$, $[CuL_2H]^{+}$, $[CuL_2]$, $[CuL_2H_{-1}]^{-}$, and $[CuL_2H_{-2}]^{2-}$ were assumed. For diglycine as ligand, the paramagnetic complex $[CuLH_{-3}]^{2-}$ was not required for a satisfactory description of the spectra up to pH = 12, but all the other species listed above were taken into consideration in the latter system. Moreover, the EPR-inactive complex $[Cu_2L_2H_{-3}]^{-}$ had to be included here in order to achieve good agreement of the metal ion concentration calculated from the spectral intensities with the analytical copper(II) concentrations (Figure 3). At equal metal and ligand concentrations, the above models resulted in good spectral fits throughout the pH range 2−12. At excess ligand, the spectra below pH = 5−6 could be described quite well, while in the neutral and alkaline regions the model had to be refined by taking into consideration the formation of additional microspecies.

Overall Equilibrium Model, Including Microequilibria. The best spectral fit can be achieved if we describe the spectra of the complexes $[CuL_2]$, $[CuL_2H_{-1}]^{-}$, and $[CuL_2H_{-2}]^{2-}$ as two-component curves, i.e., isomeric equilibria are taken into account for these species. Thus, the overall equilibrium model involves 14 EPR-active complexes for triglycine and tetraglycine, and 13 paramagnetic and 1 diamagnetic species for diglycine. The

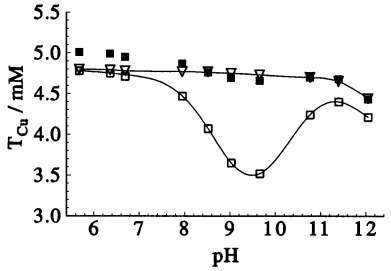

Figure 3. Analytical and calculated total copper(II) concentrations for 1:1 solutions of the copper(II)−diglycine system, where ▽ denotes the analytical metal concentration, obtained from the initial concentration and the dilution ratio, which changes together with the amount of NaOH solution added; ■ symbolizes the copper(II) concentration calculated from the mass-balance equations by using the EPR spectroscopic formation constants in Table 1; □ denotes the copper(II) concentrations calculated from the previous data, but neglecting the inactive dimer $[Cu_2L_2H_{-3}]^{-}$.

formation constants obtained from the EPR analysis, together with pH potentiometric data from the literature, are listed in Table 1. The agreement of the corresponding overall formation constants is good. The distribution of copper(II) among the various complexes is depicted in Figures 4 and 5.

Verification of the Equilibrium Model. The best model for each system results in an excellent spectral fit: the overall regression coefficients for diglycine, triglycine and tetraglycine as ligands are 0.99598, 0.99376, and 0.99515, respectively. When any species involved in the best model is neglected, the decrease in the overall regression coefficient significantly exceeds the critical value,[1] as can be seen in Table 2. The only exception is the complex $[CuL_2H_2]^{2+}$ of diglycine, where the actual decrease in R is only slightly higher than the critical value. The existence of this species is supported by the analogy with the other two systems.

The decrease in the overall regression coefficient when one or other species involved in the best model is neglected mainly originates from the significant impairment of the fit for a small group of experimental curves, whereas for a majority of the spectra the differences in fit are very small. Figure 6 illustrates the impairment of the spectral fit at excess ligand with increasing

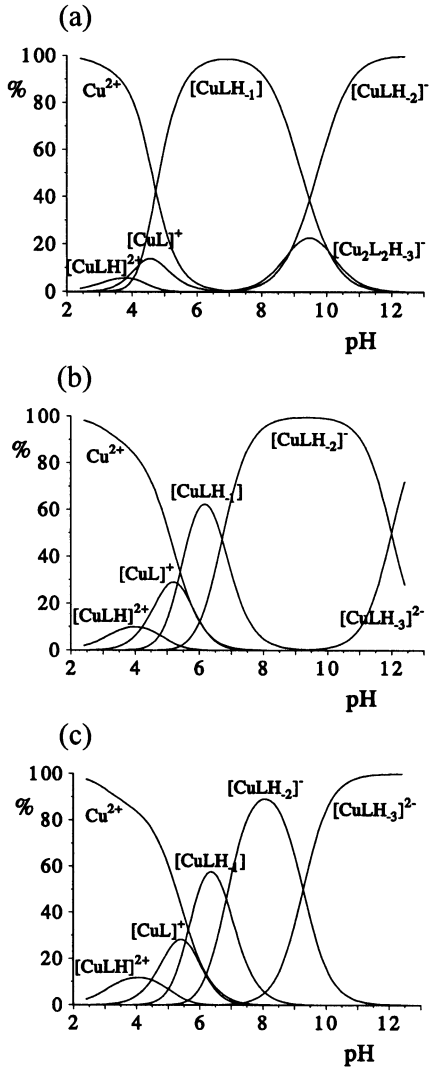

Figure 4. Concentration distribution in the (a) copper(II)−diglycine, (b) copper(II)−triglycine, and (c) copper(II)−tetraglycine systems at $T_{Cu} = T_L = 5$ mM, calculated from the EPR spectroscopic formation constants.

pH when the microequilibria for one or other of the complexes $[CuL_2]$, $[CuL_2H_{-1}]^-$, and $[CuL_2H_{-2}]^{2-}$ are not taken into consideration, i.e., the corresponding spectra are described as one-component curves.

Confidence Levels of Parameters. The EPR parameters for various complexes are presented in Table 3, whereas the component spectra calculated from them are depicted in Figure 7. The low confidence level intervals (3σ at a significance level of 99.7%) reveal the high reliability of the g_o and A_o values. For the deprotonated mono complexes, the ligand superhyperfine splitting is well-resolved (Figure 7); the confidence level of the a_{No} values here is also very good.

EPR Parameters and Coordination Modes: Mono Complexes. In the series of mono complexes, the stepwise deprotonation and equatorial coordination of peptide N donors is a typical instance of the gradual increase in ligand field that is manifested in the blue shift of the visible absorption band.[16] Simultaneously, a decrease in g_o can be observed (Table 3), in accordance with the fact that, for elongated octahedral geometry and the $d_{x^2-y^2}$ ground state of these complexes,[17] the g_o shift

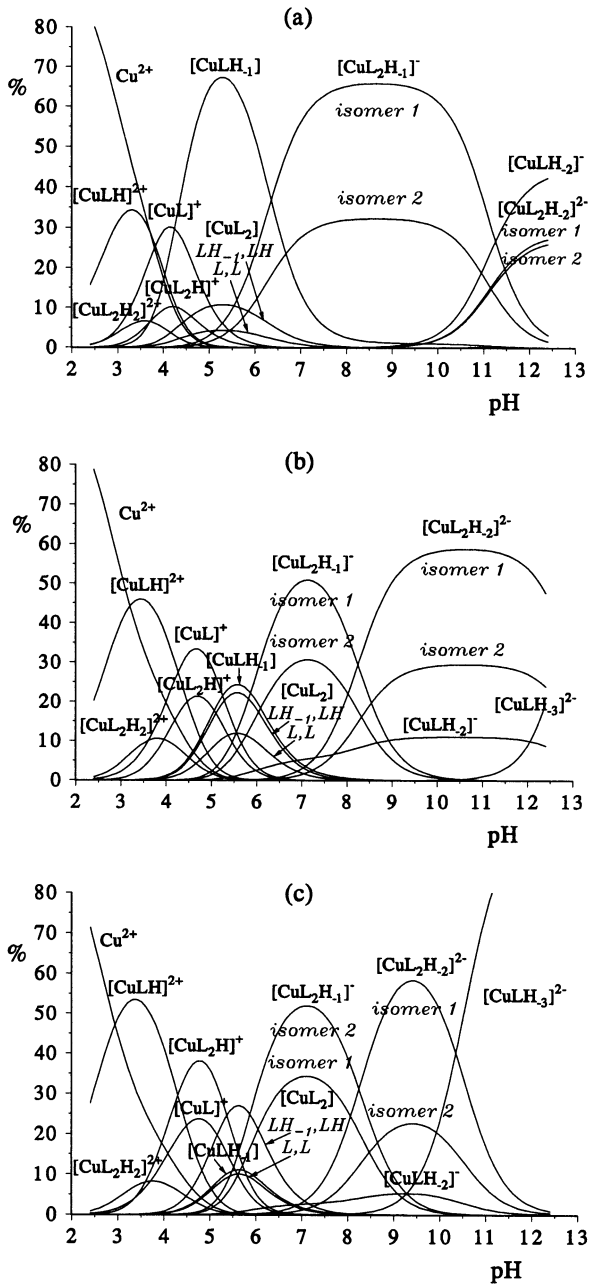

Figure 5. Concentration distribution in the (a) copper(II)−diglycine, (b) copper(II) -triglycine, and (c) copper(II) -tetraglycine systems at $T_{Cu} = 5$ mM and $T_L = 75$ mM.

mainly originates from the decrease in $g_{||}$ accompanied by the increase in energy of the $d_{xy} \leftarrow d_{x^2-y^2}$ electronic transition (which, for the above geometry, is approximately equal to the energy of the overall visible absorption band made up from the overlapping d−d bands).[1,18] Together with the decrease in g_o, A_o increases (Table 3), in accordance with the theoretical expectations for effective D_{4h} symmetry.[19] It should be stressed

(16) Sigel, H.; Martin, R. B. *Chem. Rev.* **1982**, *82*, 385−426, p 404.

(17) Szabó-Plánka, T.; Peintler, G.; Rockenbauer, A.; Györ, M.; Varga-Fábián, M.; Institórisz, L.; Balázspiri, L. *J. Chem. Soc., Dalton Trans.* **1989,** 1925−1932.

(18) Szabó-Plánka, T.; Rockenbauer, A.; Korecz, L.; Nagy, D. *Polyhedron* **2000**, *19*, 1123−1131.

(19) (a) Maki, A. H.; McGarvey, B. R. *J. Chem. Phys.* **1958**, *29*, 31−34; (b) Kivelson, D.; Neiman, R. *J. Chem. Phys.* **1961**, *35*, 149−157; (c) Goodman, B. A.; Raynor, J. B. *Adv. Inorg. Chem. Radiochem* **1970**, *13*, 135−362; (d) Peisach, J.; Blumberg, W. E. *Arch. Biochem. Biophys.* **1974**, *165*, 691−708. (e) Rockenbauer, A. *J. Magn. Reson.* **1979**, *35*, 429−438.

Table 2. Ratio of ΔR to $\Delta R_{critical}$ in the Copper(II)−Glycylglycine, Copper(II)−Triglycine, and Copper(II)−Tetraglycine Systems

		ligand		
omitted species[a]		diglycine	triglycine	tetraglycine
$[CuLH]^{2+}$		4.0	2.4	15.9
$[CuL_2H_2]^{2+}$		1.1	1.4	2.9
$[CuL_2H]^{+}$		2.2	3.8	17.0
$[CuL_2]$	2N[b]	5.0	4.3	10.7
$[CuL_2H_{-1}]^{-}$	3N[b]	7.9	1.6	10.5
	2N[b]	38.3	2.8	12.5
$[CuL_2H_{-2}]^{2-}$	4N[b]	11.0	9.1	33.4
	3N[b]	10.0	9.8	21.1

[a] For the first 3 cases, the given species was not taken into consideration at all; for the latter 3 complexes, one or other of the isomers was omitted. [b] The number of equatorial N donors in the remaining species.

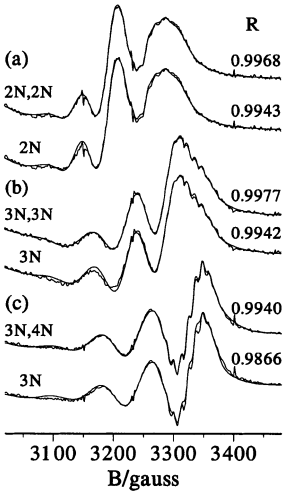

Figure 6. Experimental and calculated EPR spectra in the copper(II)−tetraglycine system at $T_{Cu} = 5$ mM and $T_L = 75$ mM, near the maximum concentration of (a) $[CuL_2]$, pH = 5.58, (b) $[CuL_2H_{-1}]^-$, pH = 7.65, and (c) $[CuL_2H_{-2}]^{2-}$, pH = 8.99. The upper spectra show the fit when the EPR curve of the complex in question is discribed as a two-component curve with the parameters in Table 3, whereas it is taken as a one-component curve for the lower spectra. In this case, the parameters are: (a) $g_o = 2.1254$, $A_o = 52.4$ G, $a_{No} = 8.0$ and 9.1 G, and α, β, and $\gamma = 39.9$, −15.9, and 9.2 G, respectively; (b) $g_o = 2.1099$, $A_o = 60.1$ G, $a_{No} = 9.1$, 9.1, and 8.1 G, and α, β, and $\gamma = 32.4$, − 21.1, and 7.0 G, respectively; and (c) $g_o = 2.0993$, $A_o = 76.4$ G, and $a_{No} = 13.2$, 13.2, and 11.2 G, and α, β, and $\gamma = 33.5$, −21.6, and 4.2G.

that axial coordination has only minor and indirect effects on g_o and A_o. The effects of peptide donor atoms, in increasing sequence, are: carboxylate O, amino N and deprotonated peptide N; the peptide O is about as weak a donor as water O, its coordination can hardly be detected by UV−vis[16] or EPR spectroscopy. This holds for OH^-, too. (The coordinating ability of the peptide O has been shown by thermodynamic studies: it forms stabil five-membered chelate rings together with the terminal amino group in copper(II)-dipeptide systems.[12,16] This mode of chelation is probable also for oligoglycines, moreover, it can reasonably be assumed that in those oligopeptide complexes where one or two peptide NH are deprotonated and bound to copper(II), the O of the subsequent peptide group also can form a weak bond with the metal ion.)

The character of the metal−ligand bonds influences g_o also by reduction of the spin−orbit coupling. The value of g_o is reduced mainly by the in-plane bonds (σ and π) through $g_{||}$.[19] There is another measure of bond character: a_{No} is proportional to the unpaired spin density at the N nuclei, so it describes the

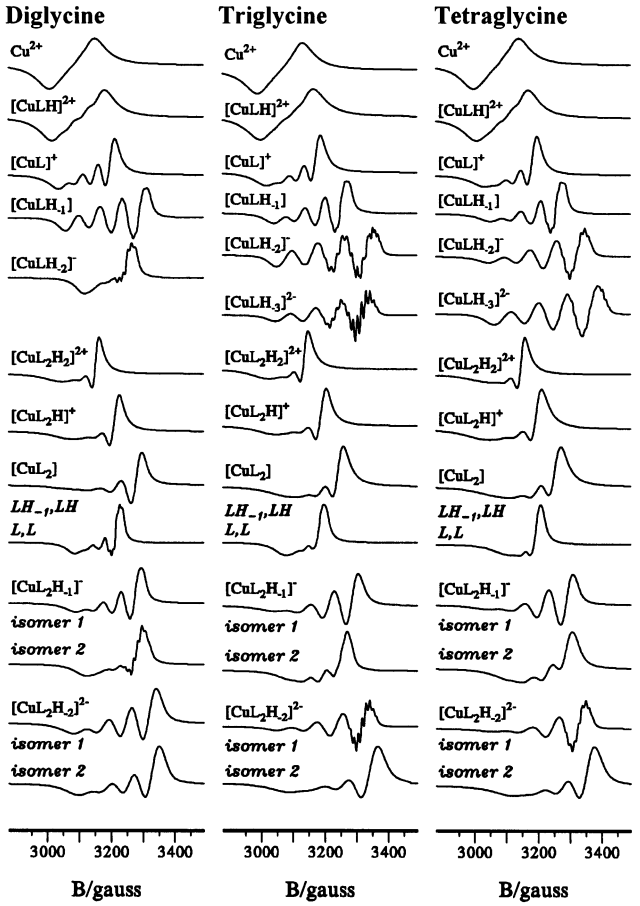

Figure 7. EPR spectra calculated from the data in Table 3 at 9.4 GHz for all paramagnetic complexes in the copper(II)−diglycine, copper(II)−triglycine, and copper(II)−tetraglycine systems.

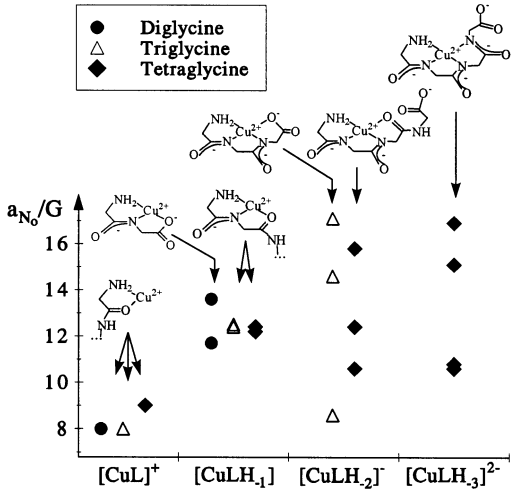

Figure 8. Superhyperfine coupling constant a_{No} of the various mono complexes, together with the corresponding coordination modes, in the copper(II)−diglycine, copper(II)−triglycine, and copper(II)−tetraglycine systems.

in-plane σ-bonds between copper(II) and N donors. It also depends on the hybridization state of the N atom: at the same degree of covalency, a lower a_{No} is expected for an sp^3 amino than for an sp^2 peptide N^- donor.[20] The a_{No} values obtained by two-dimensional EPR analysis (Table 3) are consistent with the

(20) Iwaizumi, M.; Kudo, T.; Kita, S. *Inorg. Chem.* **1986**, *25*, 1546−1550.

Table 3. ESR Parameters for the Various Complexes in the Copper(II)−Diglycine, Copper(II)−Triglycine, and Copper(II)−Tetraglycine Systems[a]

		ligand		
complex	parameters	diglycine	triglycine	tetraglycine
Cu^{2+}	g_o, A_o/G	2.1945(4), 34.5(4)	2.196(1), 34.2(9)	2.1966(2), 34.5(4)
$[CuLH]^{2+}$	g_o, A_o/G	2.1795(7), 41(2)	2.181(2), 41(2)	2.1828(1), 40(1)
$[CuL]^{+}$	g_o, A_o/G	2.1606(5), 45.8(6)	2.1647(8), 43.8(7)	2.1633(2), 42.6(5)
	a_{No}/G	8(1)	8(1)	9.0(9)
$[CuLH_{-1}]$	g_o, A_o/G	2.1198(1), 66.8(1)	2.1273(3), 59.6(3)	2.1280(1), 58.4(2)
	a_{No}/G	13.6(1), 11.7(1)	12.4(5), 12.2(5)	12.4(3), 12.2(3)
$[CuLH_{-2}]^{-}$	g_o, A_o/G	2.1164(1), 37.0(1)	2.0971(1), 80.9(2)	2.1057(1), 79.3(1)
	a_{No}/G	12.1(1), 12.1(1)	17.1(3), 14.6(2), 8.6(4)	15.8(2), 12.4(3), 10.6(2)
$[CuLH_{-3}]^{2-}$	g_o, A_o/G		2.1019(3), 78.6(4)	2.0864(1), 86.6(1)
	a_{No}/G		14.7(6), 13(1), 11.9(7)	16.9(1),15.1(1), 10.6(1),10.8(1)
$[CuL_2H_2]^{2+}$	g_o, A_o/G	2.1794(7), 34(2)	2.181(2), 35(2)	2.1797(2), 35(1)
$[CuL_2H]^{+}$	g_o, A_o/G	2.1463(7), 41(2)	2.153(1), 43(2)	2.1583(1), 46(1)
	a_{No}/G	9(5)	10(3)	11(4)
$[CuL_2]$				
isomer LH_{-1},LH	g_o, A_o/G	2.1167(7), 56(2)	2.120(1), 47(2)	2.1238(1), 51(1)
	a_{No}/G	9(2), 9(2)	9(4), 9(4)	8(4), 8(4)
isomer L,L	g_o, A_o/G	2.1386(7), 36(2)	2.144(2), 31(1)	2.1414(1), 29.4(9)
	a_{No}/G	9(1), 9(1)	9(1), 9(1)	9(1), 9(1)
$[CuL_2H_{-1}]^{-}$				
isomer 1	g_o, A_o/G	2.1148(1), 52.0(1)	2.1138(4), 68.8(4)	2.1159(1), 68.0(4)
	a_{No}/G	12.2(2), 10.6(3)	10.4(8), 8.0(6), 8.0(6)	12.7(8), 9.9(8), 7.5(9)
isomer 2	g_o, A_o/G	2.1034(2), 44.1(2)	2.1130(6), 44.2(5)	2.0983(1), 44.9(5)
	a_{No}/G	12.3(6),12.3(6),12.3(6)	14.8(6), 8(2), 8(2)	14(1), 12(2), 9.0(3)
$[CuL_2H_{-2}]^{2-}$				
isomer 1	g_o, A_o/G	2.1033(4), 66.7(6)	2.1004(2), 77.1(2)	2.1002(1), 76.5(2)
	a_{No}/G	11(1), 6.9(6), 6.9(6)	13.5(4), 12.4(7), 10.4(4)	13.8(5),12.3(3), 9.8(3)
isomer 2	g_o, A_o/G	2.0932(2), 64(1)	2.081(2), 71(3)	2.0805(3), 70(1)
	a_{No}/G	13(1), 13(1), 9(1), 9(1)	13(3), 13(3), 11(3), 11(3)	12(3), 12(3), 9(4), 9(4)

[a] The confidence intervals of the last digit (3σ) at a significance level of 99.7% are given in parentheses.

N coupling constants determined by ENDOR for related compounds.[20]

Interesting changes in a_{No} can be observed in the series of mono complexes as the numbers of deprotonated peptide groups and coupled chelate rings increase (Table 3, Figure 8). In $[CuL]^{+}$, the low value of a_{No} corresponds to the sp^3 hybridization state and a moderate bond strength. For the first deprotonation, the significant increase in a_{No} indicates the enhanced covalency of the copper(II)−N σ-bonds in all $[CuLH_{-1}]$. For the diglycine complex, there is a significant difference between the two N donors, while for the other ligands, the a_{No} values agree within experimental error. We explain this in terms of the different nature of the third donor: the carboxylate group, a strong donor, can bind strongly and stabilize the adjacent copper(II)−peptide N^{-} bond in the diglycine complex, which is manifested in a larger value of the corresponding a_{No}. In contrast, the partial coordination of the weak peptide O in the triglycine and tetraglycine complexes has a much weaker effect. The difference in the third donor group is reflected in the g_o values, too (Table 3). The deprotonation of the second peptide NH is accompanied by extremely high values of a_{No}, especially for the complex $[CuLH_{-2}]^{-}$ of triglycine (Table 3), and the explanation can be similar to that in the former case: the deprotonation and coordination of the second peptide N further stabilizes the first copper−peptide N^{-} bond, increasing the corresponding N coupling constant. For $[CuLH_{-2}]^{-}$ of triglycine, the stabilizing effect of the terminal carboxylate group bound in the fourth position is added, leading to unusually high a_{No} values (most probably for the peptide N atoms) (Figure 8) and to a decrease in g_o (Table 3). For the complex $[CuLH_{-3}]^{2-}$ of tetraglycine, the third deprotonated peptide group seems to play a similar stabilizing role to that of the carboxylate group in the former species: two very high superhyperfine coupling constants (and considerably lower g_o) are found again. The above statements can be summarized as follows: when a N atom takes part simultaneously in the formation of two adjacent chelate rings, and two neighboring donors are bound strongly to the copper(II) ion as well, then the in-plane σ-bond between the N atom and the metal ion becomes particularly strong. Here, we have found EPR spectroscopic evidence for a significant stabilizing effect in complexes with several coupled chelate rings.

It is generally accepted that the water molecule at the fourth equatorial site of $[CuLH_{-1}]$ is deprotonated when the mixed hydroxo complex $[CuLH_{-2}]^{-}$ of diglycine is formed. This is accompanied by a small decrease in g_o (Table 3), though a_{No} (of two equivalent N donors here) is smaller than in $[CuLH_{-1}]$. The less covalent copper−N σ-bonds seem to be compensated by more covalent π-bonds; competition between various metal−ligand bonds has been observed for many other copper(II) complexes,[21] too. Another effect of OH^{-} is a dramatic decrease in the copper(II) coupling constant (Table 3), which can be explained by 3d−4s orbital mixing as a consequence of a rhombic distortion induced by repulsion between the OH^{-} and the neighboring carboxylate group.[14d]

For the mixed hydroxo complex $[CuLH_{-3}]^{2-}$ of triglycine, a small but significant g_o shift indicates modified equatorial coordination as compared to $[CuLH_{-2}]^{-}$: in the case of axial ligation of the weak OH^{-}, no significant change in g_o is expected. If OH^{-} replaces the carboxylate group, an increase

(21) Lukaš, M.; Kývala, M.; Hermann, P.; Lukeš, I.; Sanna, D.; Micera, G. *J. Chem. Soc., Dalton Trans.* **2001**, 2850−2857.
(22) Zékány, L; Nagypál, I; Peintler, G.: PSEQUAD for Chemical Equilibria, Technical Software Distributors, Baltimore, MD, 1991.

of 0.005−0.01 in g_o is expected (the carboxylate group is not bound in the complexes $[CuLH_{-1}]$ of triglycine and tetraglycine, and g_o is higher by 0.007 and 0.008, respectively, than for the corresponding diglycine complex with equatorial carboxylate coordination (Table 3)), and this increase may be counterbalanced in part by the equatorial ligation of OH^- (the latter ligand decreased g_o by 0.004 in the analogous diglycine complexes). Thus the increase of 0.005 in g_o supports the equatorial coordination of OH^- in the complex $[CuLH_{-3}]^{2-}$ of triglycine, in accordance with the facts that (1) g_o is smaller by about 0.004 for this complex than for the complex $[CuLH_{-2}]^-$ of tetraglycine, where the fourth equatorial site is partially occupied by a weak peptide O (Figure 8), and (2) the differences in the N coupling constants are much less than for the complex $[CuLH_{-2}]^-$ (Table 3), pointing to a break-down of the stabilization effect of the chelating carboxylate group.

Bis Complexes. For $[CuL_2H_2]^{2+}$, a high g_o corresponds to (LH + LH) coordination through the carboxylate groups (Table 3). For $[CuL_2H]^+$, an (LH + L) binding mode is most probable, where the ligand L is connected to the metal ion via its amino N and peptide O atoms, as in $[CuL]^+$, whereas the other peptide is ligated through its carboxylate group (Figure 9). The g_o values correspond to the above donor sets in each system (Table 3).

As the g_o values of the two isomers of $[CuL_2]$ differ significantly (by 0.018−0.024 in the various systems, Table 3), different equatorial donor atom sets rather than different arrangements of the same donors are most probable. The g_o values of the major isomers are somewhat lower than those of the corresponding complexes $[CuLH_{-1}]$, suggesting similar modes of coordination, supplemented by an additional, not very strong donor. Accordingly, an (LH_{-1} + LH)-type binding mode is likely here, where the second ligand has its amino group protonated and is connected to the $CuLH_{-1}$ moiety via its carboxylate group. The higher g_o values of the minor microspecies correspond to (L + L) coordination by the amino N and peptide O atoms (Figure 9).

For $[CuL_2H_{-1}]^-$, different isomer pairs have been found with the various ligands. In the case of the diglycine complex, the significant difference in g_o indicates different equatorial donor atom sets in the microspecies: the higher g_o of the major isomer is nearly equal to that of $[CuLH_{-1}]$, suggesting a similar equatorial donor atom set, while the significantly lower g_o of the minor isomer (Table 3) suggests a stronger ligand field. In accordance with earlier thermodynamic studies,[12] this indicates that the tridentate equatorial coordination of the deprotonated ligand persists in $[CuL_2H_{-1}]^-$, and an additional chelate ring is formed by the ligand L bound in equatorial-axial positions through the amino N and peptide O atoms. The isomers differ from each other in the positions of the latter donors: the fourth equatorial site in the major isomer with higher g_o is occupied by the weak peptide O, whereas in the minor microspecies with lower g_o, it is occupied by the amino N (Figure 9). The low g_o of these species would be accompanied by a fairly high copper hf coupling constant if the effective D_{4h} symmetry were preserved (cf. the mono complexes, Table 3). However, A_o is low, especially for the minor isomer, where the amino groups occupy neighboring sites. This indicates that rhombic distortion is induced by the equatorial-axial ligation of the second ligand, which is enhanced by the interaction between the amino groups in close vicinity to each other.

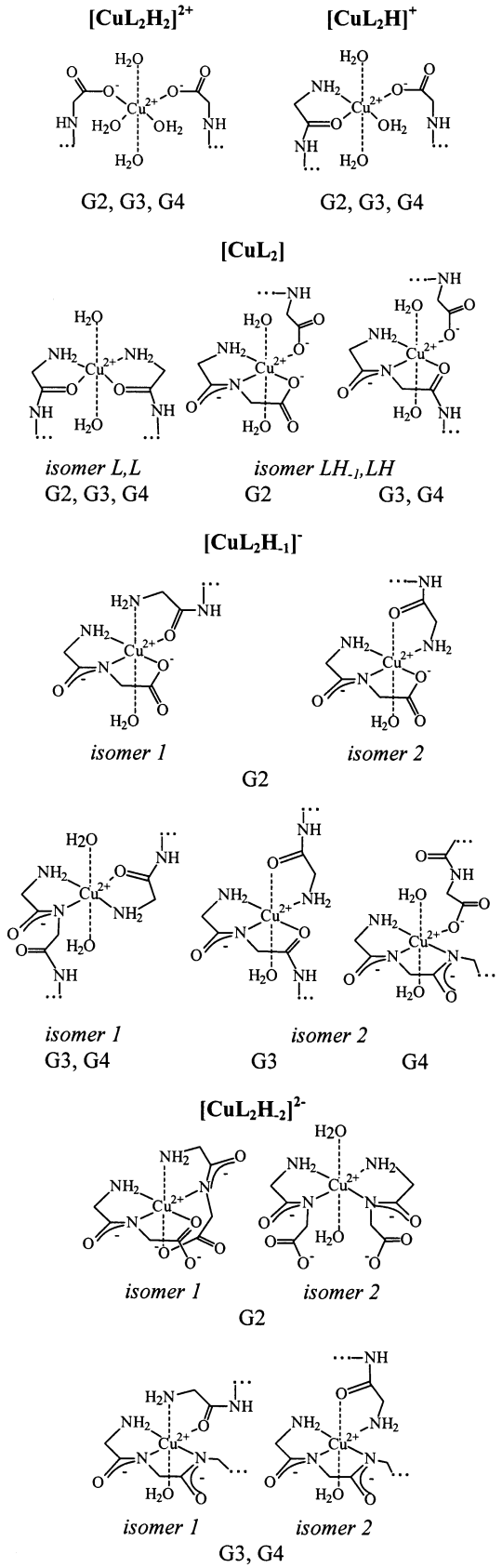

Figure 9. Coordination modes proposed for the various bis complexes in the copper(II)−diglycine (G2), copper(II)−triglycine (G3), and copper(II)−tetraglycine (G4) systems.

For the triglycine complex, (LH_{-2} + LH) coordination may occur in principle, but it is less probable since a tridentate +

monodentate ligation of 2 ligands is less preferred than the very stable tetradentate binding of 1 ligand by the same equatorial donor atom set, found in $[CuLH_{-2}]^-$. The EPR data offer further evidence: (1) similar $g_{\ddot{o}}$ values suggest identical donor atom sets in the isomers, but (LH_{-2} + LH) coordination would not allow different arrangements of donors; (2) the g_o values point to a somewhat stronger ligand field than in $[CuLH_{-1}]$ of triglycine, and thus (LH_{-1} + L) coordination with equatorial binding of the amino group of ligand L and different arrangements of the donor atoms is most probable. The not too low A_o value of the major isomer does not indicate significant rhombic distortion, so diequatorial coordination of both ligands with the trans position of the amino groups (Figure 9) is likely in this species. For the minor isomer, in turn, the low copper hyperfine coupling constant suggests considerable deviation from effective D_{4h} symmetry. We explain this by the cis position of the amino groups, which is promoted by the (partial) coordination of the peptide O of the deprotonated tripeptide when the equatorial-axial binding of ligand L occurs (Figure 9). (It should be noted, however, that the EPR data do not allow the exclusion of the diequatorial coordination of both ligands in this microspecies.)

For the tetraglycine complex, the g_o and A_o of isomer 1 agree within experimental error with the corresponding parameters of the major isomer of the analogous triglycine complex (Table 3); thus, the same mode of coordination is most probable (Figure 9). In contrast with the triglycine complex, however, this microspecies is the minor one here. The major isomer has much a lower g_o, reflecting a much stronger ligand field (Table 3). g_o is lower by 0.008 than that of $[CuLH_{-2}]^-$, which corresponds to an amino N + 2 deprotonated peptide N^- equatorial donor atom set from a ligand LH_{-2}, completed with the equatorially bonded carboxylate O of the peptide in the protonated state LH (Figure 9).

The $[CuL_2H_{-2}]^{2-}$ of diglycine can be formed either by proton loss from the ligand L of $[CuL_2H_{-1}]^-$, or by OH^- coordination to $[CuL_2H_{-1}]^-$. The low g_o values support the former case (Table 3). Accordingly, in the minor microspecies with lower g_o, diequatorial ligation of both ligands via their amino and deprotonated peptide groups is most likely (4N isomer). For this low g_o, a much higher A_o would be expected in the event of effective D_{4h} symmetry. The low copper coupling constant can be attributed to rhombic distortion induced by the lower-symmetry cis arrangements of the donors of the same kind (Figure 9). The higher g_o of the other isomer indicates a weaker ligand field; this can be explained by the assumption of tridentate equatorial coordination of the first ligand via its amino, deprotonated peptide and carboxylate groups, which leaves only one equatorial position free for the other dipeptide (3N isomer). It is therefore the deprotonated peptide N^- of the second ligand that occupies the fourth site, as metal-ion-induced deprotonation requires the formation of a strong bond between the metal ion and the deprotonated donor. In this way, the amino and carboxylate groups of the second dipeptide can occupy only axial positions (Figure 9).

The considerably different g_o values for the isomers of $[CuL_2H_{-2}]^{2-}$ of triglycine and tetraglycine similarly point to different equatorial donor atom sets, excluding cis−trans isomerism of (LH_{-1} + LH_{-1}) coordination. For the minor isomer, g_o is even lower than that for the 4N isomer of the corresponding diglycine complex, though the strongest possible donor atom set is the same for both (2 amino N + 2 deprotonated peptide N^- atoms). The significantly smaller g_o for the complexes of triglycine and tetraglycine (Table 3) most probably indicates even more covalent metal−ligand bonds stabilized by coupled chelate rings, i.e., (LH_{-2} + L) coordination (Figure 9). The amino groups are forced into the cis position by the triequatorial binding of the deprotonated ligand, which is manifested in rhombic distortion and a reduced A_o.

For the major isomer, g_o is too high for (LH_{-1} + LH_{-1}) coordination and the diequatorial ligation of both ligands (Table 3, cf. the 4N isomer of the diglycine complex), whereas it is close to the g_o of $[CuLH_{-2}]^-$. Therefore, (LH_{-2} + L) coordination is suggested again, though here the fourth equatorial site is occupied not by the amino N, but by the peptide O of ligand L (Figure 9).

The much higher deprotonation pK of $[CuL_2H_{-1}]^-$ of diglycine (11.34 from data in Table 1) as compared to the corresponding complexes of the two other ligands (pK = 8.21 and 8.32) can be understood if it is considered that the deprotonation of both ligands is necessary for formation of the diglycine complex. At the same time, the carboxylate group promotes the strong tridentate ligation of the first ligand, which in turn inhibits the coordination of the second ligand: the formation of the 4N isomer requires the breakdown of the tridentate binding of the first ligand, while for the formation of the 3N isomer, the anchoring amino group can form only a weak axial bond with the metal ion. Our experience and this explanation for the higher deprotonation pK of the above diglycine complex are in accord with the results of Lukaš et al.,[21] obtained with substituted primary phosphinic acid ligands analogous to diglycine.

Conclusions

The two-dimensional EPR evaluation method allowed an integrated description of the very complicated copper(II)−oligoglycine systems, offering data on the microspeciation and coordination modes for 14 metal complexes.

For the mono complexes, structures involving coupled chelate rings are stabilized by particularly strong copper(II)−N in-plane σ-bonds. For the bis complexes, the formation of coupled chelate rings is also favored: (1) The tridentate equatorial ligation of the ligand LH_{-1} makes the complex $[CuL_2H_{-1}]^-$ of diglycine predominant in a wide pH range, inhibiting the microprocesses leading to the formation of $[CuL_2H_{-2}]^{2-}$. (2) In the major isomer of $[CuL_2H_{-1}]^-$ of tetraglycine, (LH_{-2} + LH) coordination occurs. (3) The predominant mode of coordination in both isomers of $[CuL_2H_{-2}]^{2-}$ of triglycine and tetraglycine is (LH_{-2} + L).

Experimental Section

Reagents and Solutions. The oligoglycine ligands (denoted by HL in their neutral forms) from Sigma and other reagents from Reanal (Hungary) were of analytical grade and were used without further purification. The total copper(II) concentration T_{Cu} of the solutions was 5 mM, while the total ligand concentrations T_L were 5 mM or 75 mM. We used 0.2 M KCl as background electrolyte. The pH was adjusted with HCl, and then with NaOH, to an accuracy of 0.01 pH unit, using a Radiometer PHN 240 pH meter equipped with a Radiometer GK2401C combined glass electrode. The electrode was calibrated with IUPAC Standard Buffers from Radiometer. The formation constant for the complex $[Cu_pL_qH_r]$ is defined as the equilibrium constant for the

process $p \cdot Cu + q \cdot L + r \cdot H \rightleftharpoons [Cu_pL_qH_r]$. (The ligands in their neutral forms are denoted by [LH]: $p = 0$, $r = q = 1$.)

EPR Measurements. A 10 cm^3 stock solution was titrated under an argon atmosphere. The sample was mixed by bubbling the gas through the solution. A Masterflex CL peristaltic pump ensured the circulation (14 $cm^3\ min^{-1}$) of the solution through the capillary tube in the cavity. The EPR spectra were taken after circulation for 2 min at the chosen pH at room temperature (291 K) on an upgraded JEOL JES−FE3X spectrometer with 100 kHz field modulation, using a manganese(II)-doped MgO powder for the calibration of g. Further details of the measurements were described in a previous paper.[14]

The parameters for the aqua complex were determined independently, too, in the absence of ligand at 5 mM copper(II) chloride and 0−0.4 M KCl concentration. The parameters of the aqua complex were found to be independent of the concentration of the background electrolyte.

Evaluation of Spectra. For the experimental EPR spectra, we eliminated the background signal by subtracting the "glass signal", which contained the vanadium signal of the Pyrex tube and the Mn peaks of the Mn:MgO external standard. To compensate the minor frequency shifts in the course of measurements, the field scale was shifted to secure a perfect fit for the Mn lines of the external standard.

Matrix Rank Analysis. The number of independent active species was determined by calculating the residual intensity curves with the MRA program.[15]

Decomposition of Spectra. The series of spectra were evaluated with the 2D_EPR program.[1] Each component curve was described by the parameters g_o, the copper and ligand hyperfine coupling constants A_o and a_{No}, respectively, and the relaxation parameters α, β, and γ, which are related to the widths of the copper lines as $\sigma_{M_I} = \alpha + \beta M_I + \gamma M_I^2$ (M_I is the magnetic quantum number of copper nuclei). Since the copper(II) (as chloride) used to make the stock solution was a natural mixture of isotopes, the spectrum of each species was calculated as the sum of spectra containing ^{63}Cu and ^{65}Cu weighted by their abundances in nature. The copper and ligand coupling constants and the field dimension relaxation parameters are given in gauss (G) units throughout the paper; 1 G = 10^{-4} T.

Acknowledgment. We thank the Hungarian Scientific Research Fund OTKA (Grants Nos. T-032929 and T-029838) for financial support. We are indebted to Dr. David Durham for stylistic correction of the manuscript.

Supporting Information Available: Figure illustrating the impairment of spectral fit when one or other of the species $[CuLH]^{2+}$, $[CuL_2H_2]^{2+}$, and $[CuL_2H]^{+}$ is omitted, and the overall EPR parameter sets including relaxation parameters for various complexes. This material is available free of charge via the Internet at http://pubs.acs.org.

JA021245+